The Astrophysical Journal, 608:10–15, 2004 June 10

FIRST YEAR *WILKINSON MICROWAVE ANISOTROPY PROBE* OBSERVATIONS: DARK ENERGY INDUCED CORRELATION WITH RADIO SOURCES

M. R. Nolta,[1] E. L. Wright,[2] L. Page,[1] C. L. Bennett,[3] M. Halpern,[4] G. Hinshaw,[3] N. Jarosik,[1] A. Kogut,[3] M. Limon,[3,5] S. S. Meyer,[6] D. N. Spergel,[7] G. S. Tucker,[8,5] and E. Wollack[4]

Received 2003 May 7; accepted 2004 February 23

ABSTRACT

The first-year *Wilkinson Microwave Anisotropy Probe* (*WMAP*) data, in combination with any one of a number of other cosmic probes, show that we live in a flat Λ-dominated cold dark matter (CDM) universe with $\Omega_m \approx 0.27$ and $\Omega_\Lambda \approx 0.73$. In this model the late-time action of the dark energy, through the integrated Sachs-Wolfe effect, should produce cosmic microwave background (CMB) anisotropies correlated with matter density fluctuations at $z \lesssim 2$ (Crittenden & Turok 1996). The measurement of such a signal is an important independent check of the model. We cross-correlate the NRAO VLA Sky Survey (NVSS) radio source catalog (Condon et al. 1998) with the *WMAP* data in search of this signal, and see indications of the expected correlation. Assuming a flat ΛCDM cosmology, we find $\Omega_\Lambda > 0$ (95% CL, statistical errors only) with the peak of the likelihood at $\Omega_\Lambda = 0.68$, consistent with the preferred *WMAP* value. A closed model with $\Omega_m = 1.28$, $h = 0.33$, and no dark energy component ($\Omega_\Lambda = 0$), marginally consistent with the *WMAP* CMB TT angular power spectrum, would produce an anticorrelation between the matter distribution and the CMB. Our analysis of the cross-correlation of the *WMAP* data with the NVSS catalog rejects this cosmology at the 3 σ level.

Subject headings: cosmic microwave background — cosmology: observations

1. INTRODUCTION

The recent *Wilkinson Microwave Anisotropy Probe*[9] results (*WMAP*; Bennett et al. 2003c) place on a firm foundation the emerging standard model of cosmology: a flat adiabatic Λ-dominated cold dark matter (CDM) universe. However, the deficit of power in the cosmic microwave background (CMB) anisotropy spectrum on large angular scales (Bennett et al. 2003a; Hinshaw et al. 2003; Spergel et al. 2003) is surprising given that ΛCDM models predict an enhancement at $\ell \lesssim 10$ due to the late-time integrated Sachs-Wolfe (ISW) effect (Sachs & Wolfe 1967). The likelihood of observing so little power because of sample variance is only 0.15% (Spergel et al. 2003). Thus, new physics may be indicated since the nature of the dark energy is poorly understood. Cross-correlating the CMB with radio sources provides a direct test for the recent acceleration predicted by the favored ΛCDM model and observed by the Type 1a supernovae experiments (Perlmutter et al. 1999; Riess et al. 1998). Thus, this test is an important check of the standard model.

Any recent acceleration of the universe will cause local gravitational potentials to decay. This decay is then imprinted on the CMB since the photons, which were blueshifted on infall, suffer less of a redshift as they climb out of the potential well. This produces temperature perturbations

$$\frac{\delta T(\hat{n})}{T_0} = -2 \int_0^{\eta_{\rm dec}} d\eta \, \frac{d\Phi}{d\eta}(\eta \hat{n}), \tag{1}$$

where Φ is the Newtonian gravitational potential, η is the conformal look-back time, and the integral runs from today ($\eta = 0$) to the CMB decoupling surface at $z_{\rm dec} = 1089$. Figure 1 shows the recent evolution of Φ for a variety of cosmological models. Since Φ is related to the matter distribution via the Poisson equation, tracers of the mass will be correlated with the CMB through the late ISW effect (Crittenden & Turok 1996; Peiris & Spergel 2000). In this paper, we correlate the NRAO VLA Sky Survey (NVSS) source catalog (Condon et al. 1998) with the *WMAP* CMB map in search of the late ISW effect. We focus on the implications of this correlation for dark energy, specifically Ω_Λ. Boughn & Crittenden (2002) performed a similar analysis using the *COBE* DMR map, and found no correlation. However, a recent reanalysis by the same authors using the *WMAP* data did see evidence for a correlation between the CMB, NVSS, and the hard X-ray background observed by the *HEAO 1* satellite (Boughn & Crittenden 2004). Several other groups have reported detecting correlations between *WMAP* and the Automatic Plate Measuring Facility (APM) and Sloan Digital Sky Survey (SDSS) galaxy catalogs (Fosalba & Gaztanaga 2004; Fosalba et al. 2003; Scranton et al. 2004).

We take as our fiducial model the best-fit power-law ΛCDM model to the combined *WMAP*, CBI (Cosmic Background Imager), ACBAR (Arcminute Cosmology Bolometer Array Receiver), 2dFGRS (Two-Degree Field Galaxy Redshift Survey), and Lyα data sets, with values $\omega_m = 0.133$, $\omega_b = 0.0226$, $n_s = 0.96$, $h = 0.72$, $A = 0.75$, and $\tau = 0.117$ (Spergel et al.

[1] Department of Physics, Jadwin Hall, Princeton University, Princeton, NJ 08544; mrnolta@princeton.edu.
[2] UCLA Astronomy, P.O. Box 951562, Los Angeles, CA 90095-1562.
[3] Code 685, NASA Goddard Space Flight Center, Greenbelt, MD 20771.
[4] Department of Physics and Astronomy, University of British Columbia, Vancouver, BC V6T 1Z1, Canada.
[5] National Research Council (NRC) Fellow.
[6] Departments of Astrophysics and Physics, Enrico Fermi Institute and Center for Cosmological Physics, University of Chicago, Chicago, IL 60637.
[7] Department of Astrophysical Sciences, Princeton University, Princeton, NJ 08544.
[8] Department of Physics, Brown University, Providence, RI 02912.
[9] *WMAP* is the result of a partnership between Princeton University and the NASA Goddard Space Flight Center. Scientific guidance is provided by the *WMAP* Science Team.

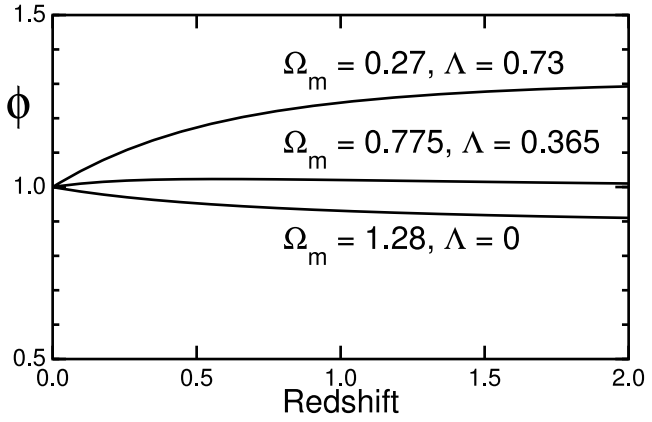

FIG. 1.—Gravitational potential Φ as a function of redshift z for a variety of cosmological models. The models are normalized to unity at $z = 0$.

2003, Table 7); the implied value for Ω_Λ is 0.74. Cosmological parameters are drawn from this set unless otherwise noted.

In § 2, we briefly describe the NVSS source catalog and its autocorrelation function (ACF). In § 3, we describe the cross-correlation between the *WMAP* CMB map and the NVSS source map, and relate it to the late-ISW effect. We conclude in § 4 and discuss effects which could mimic the observed signal.

2. THE NVSS SOURCE CATALOG

The NVSS is a 1.4 GHz continuum survey, covering the 82% of the sky that has $\delta > -40^\circ$ (Condon et al. 1998). The source catalog contains over 1.8×10^6 sources and is 50% complete at 2.5 mJy. Nearly all the sources away from the Galactic plane ($|b| > 2^\circ$) are extragalactic. The bright sources are predominantly AGN-powered radio galaxies and quasars, while at weaker fluxes the sources are increasingly nearby star-forming galaxies.

Galaxy counts are a potentially biased tracer of the underlying matter distribution, and thus the projected number density of NVSS sources per steradian, $n(z, \hat{n})$, is related to the matter distribution $\delta(z, \hat{n}) \equiv \delta\rho/\rho$ via

$$n(z, \hat{n})\, dz\, d\Omega = \frac{dN}{dz}\left[1 + b_r(z)\delta(z, \hat{n})\right] dz\, d\Omega, \qquad (2)$$

where dN/dz is the mean number of sources per steradian at a redshift z and $b_r(z)$ is the radio galaxy bias parameter. Thus, the observed fluctuation on the sky in projected source counts is given by

$$\delta N(\hat{n}) = \int dz\, b_r(z) \frac{dN}{dz} \delta(z, \hat{n}). \qquad (3)$$

Since we are only interested in clustering on large scales, and hence the linear regime, the evolution of δ factors as $\delta(k, z) = D(z)\delta(k)$, where $\delta(k, z)$ is the Fourier transform of the matter distribution, $\delta(k) \equiv \delta(k, 0)$ its current value, and $D(z)$ is the linear growth factor (Peebles 1993, § 5.111). While generally a function of time, we take the bias to be constant since the determination of dN/dz is uncertain and we only consider a modest redshift range ($0 < z < 2$).

While the individual NVSS source redshifts are unknown, for our purposes we need only the overall redshift distribution dN/dz for the NVSS. We adopt the favored model of Dunlop & Peacock (1990, hereafter DP90; model 1, MEAN-z data), which was found by Boughn & Crittenden (2002) to best reproduce the NVSS ACF. In common with most models, it divides the sources by spectral index α (flux $S \propto \nu^{-\alpha}$) into two populations; flat-spectrum ($\alpha \approx 0$) and steep-spectrum ($\alpha \approx 0.8$) sources. The model is plotted in Figure 2. We limit the model to $0.01 < z < 5$; the lower limit corresponds to a distance of ≈42 Mpc . The small peak at $z \approx 0.05$ is spurious (because of a breakdown in the DP90 fitting function), but has only a minor effect on the integrated predictions.

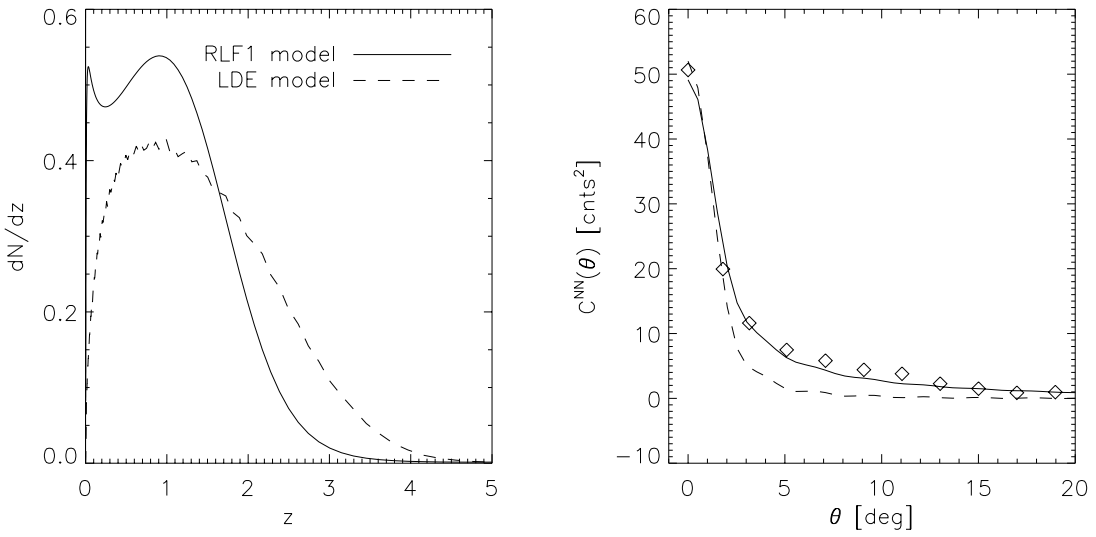

FIG. 2.—Adopted dN/dz model (RLF1) for the distribution of NVSS sources from DP90, normalized to integrate to unity (*left panel*). The small blip at $z \approx 0.05$ is spurious and is due to breakdown in the DP90 fitting function. Also plotted is the "luminosity/density evolution" (LDE) model also from DP90, which is a poor fit to the observed ACF (*right panel*).

Given a cosmology, we can determine the radio bias b_r from the amplitude of the NVSS ACF by comparing the ACF to the unbiased prediction

$$C^{NN}(\theta) = \langle \delta N(\hat{n}) \delta N(\hat{n}') \rangle = \sum \frac{2l+1}{4\pi} [b_l^N]^2 C_l^{NN} P_l(\hat{n} \cdot \hat{n}'), \quad (4)$$

where $[b_l^N]^2$ is the pixel window function. Substituting equation (3) into this expression and Fourier transforming,

$$C_l^{NN} = 4\pi \int \frac{dk}{k} \Delta_\delta^2(k) \left[f_l^N(k) \right]^2, \quad (5)$$

where $\Delta_\delta^2(k) = k^3 P_\delta(k)/2\pi^2$ is the logarithmic matter power spectrum and $P_\delta(k) = \langle |\delta(k)|^2 \rangle$. We use the *WMAP* normalization $\Delta_{\mathcal{R}}^2(k_0) = 2.95 \times 10^{-9} A$, where $k_0 = 0.05$ Mpc^{-1} (Verde et al. 2003), giving us $\delta_H = 6.1 \times 10^{-5}$ for our fiducial model. The filter function is given by

$$f_l^N(k) = b_r \int dz \, \frac{dN}{dz} D(z) j_l(k\eta), \quad (6)$$

where $j_l(x)$ is the spherical Bessel function. Note that the bias we measure is complicated by the uncertainty in dN/dz; errors in the normalization are absorbed into the bias.

To calculate the observed NVSS ACF, we made a HEALPix (Górski et al. 1999) resolution-5 map of $\delta N(\hat{n})$, which has 12,288 $1.^\circ 8 \times 1.^\circ 8$ pixels.[10] As a precaution, we removed the 3×10^5 resolved sources from the catalog. The mean source count per pixel is 147.9, leading to a Poisson uncertainty of $\approx$8%. The ACF is estimated as

$$\hat{C}^{NN}(\theta_k) = \frac{\sum N_i N_j w_i^N w_j^N}{\sum w_i^N w_j^N}, \quad (7)$$

where N_i is the number of sources in pixel i and the sum is over all pixel pairs separated by $\theta_k - \Delta\theta/2 < \theta < \theta_k + \Delta\theta/2$. The bin width $\Delta\theta$ is 2°. We mask out pixels at low Galactic latitude ($|b| < 10^\circ$) and those unobserved by the survey ($\delta < -37^\circ$); the weights w_i^N are determined by the mask. The NVSS ACF is shown is Figure 2. The $\theta = 0^\circ$ bin is corrected for Poisson noise by subtracting the mean number of sources per pixel. For the fiducial model parameters [which are used to calculate $D(z)$ and $\eta(z)$], the derived bias is 1.7. This is somewhat higher than the value of 1.6 found by Boughn & Crittenden (2002). However, they assumed a scale-invariant spectrum (i.e., $n_s = 1$), and changing n_s by ± 0.03 changes the bias by ∓ 0.05.

As noticed by Boughn & Crittenden (2002), the NVSS catalog mean source density varies with declination, introducing a spurious signal into the ACF. They corrected for this by adding and subtracting random sources from the map until the structure was removed. We considered two simple corrections; both broke the sources into $\sin(\delta)$ strips of width 0.1. The first method subtracted the mean from each strip; the second scaled each strip by the ratio of the global mean to the strip mean. Since the corrections are small, both produced similar results (Fig. 3).

[10] For more information on HEALPix visit http://www.eso.org/science/healpix/. The *resolution* of a HEALPix map indicates its pixel count. A resolution-r map has $12N_{\rm side}^2$ pixels, where $N_{\rm side} = 2^r$. A resolution-$(r+1)$ map is created by dividing each resolution-r pixel into four subpixels.

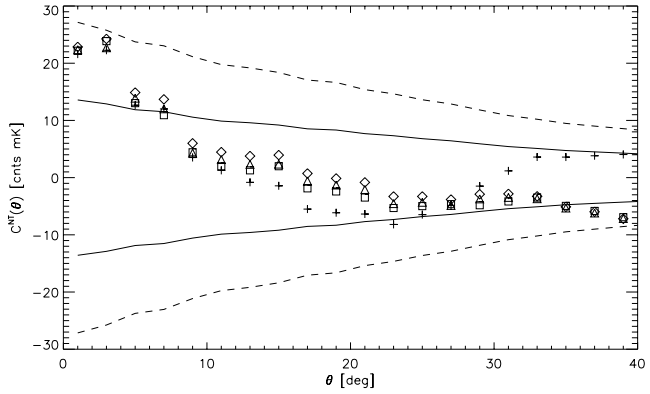

FIG. 3.—*WMAP*-NVSS CCF. The CCF is insensitive to the details of the declination correction. Two simple methods are compared; both broke the sources into $\sin(\delta)$ strips of width 0.1. The first (*diamonds*) subtracted the mean from each strip. The second (*triangles*) scaled each strip by the ratio of the global mean to the strip mean. The cross points are uncorrected, showing the correction is only important for $\theta \gtrsim 25$. We used the *WMAP* ILC CMB map; substituting the map of Tegmark et al. (2003) instead produces the same results (*squares*). The solid and dashed lines are derived from the diagonal elements of the correlation matrix because of accidental alignments; they would be the 1 σ and 2 σ contours in the absence of off-diagonal correlations. The points, however, are highly correlated, as shown in Table 1.

3. *WMAP*–NVSS CROSS-CORRELATION

Combining equations (1) and (3), we can calculate the expected cross-correlation spectrum between the NVSS catalog and the CMB:

$$C_l^{NT} = \langle a_{lm}^N a_{lm}^{T*} \rangle = 4\pi \int \frac{dk}{k} \Delta_\delta^2(k) f_l^N(k) f_l^T(k), \quad (8)$$

where f_l^N and f_l^T are the NVSS and ISW filter functions. The ISW filter function is derived analogously to the NVSS filter function. The local gravitational potential is related to the matter distribution via the Poisson equation $\nabla^2 \Phi = 4\pi G a^2 \rho_m \delta_m$, where the gradient is taken with respect to comoving coordinates. Fourier transforming, we have

$$\Phi(k, \eta) = -\frac{3}{2} \Omega_m \left(\frac{H_0}{k} \right)^2 g(\eta) \delta(k), \quad (9)$$

where H_0 is the Hubble constant, $\Omega_m H_0^2 = 8\pi G \rho_m^0/3$, and $g(\eta) \equiv D(\eta)/a(\eta)$ is the linear growth suppression factor. Thus,

$$f_l^T(k) = 3\Omega_m \left(\frac{H_0}{k} \right)^2 \int d\eta \, \frac{dg}{d\eta} j_l(k\eta). \quad (10)$$

We use the fitting function for $g(\eta)$ provided by Carroll et al. (1992). In a flat $\Omega_m = 1$ universe, $g(\eta)$ is constant and thus there is no ISW effect and hence no correlation between the CMB and the local matter distribution. In ΛCDM universes, $D(\eta)$ approaches a constant during Λ-domination, leading to a decay of $g(\eta)$ as time increases.

We computed the *WMAP*-NVSS cross-correlation function (CCF) as

$$\hat{C}^{NT}(\theta_k) = \frac{\sum N_i T_j w_i^N w_j^T}{\sum w_i^N w_j^T}, \quad (11)$$

TABLE 1
WMAP-NVSS CCF Correlation Matrix

Bin	1°	3°	5°	7°	9°	11°	13°	15°	17°	19°
1°	183	159	141	131	115	98.7	87	73.7	58.7	49.7
3°	...	161	140	136	119	104	94.3	82.8	67.6	59.6
5°	...	...	135	128	113	97.8	86.4	74.8	60.4	52.5
7°	...	...	...	135	120	106	96.7	86.4	71.9	64.2
9°	...	...	...	...	113	102	92.6	83.7	70.3	63.4
11°	...	...	...	...	...	95.9	89.2	81.6	69.6	63.5
13°	...	...	...	...	...	...	88.3	82.7	71.7	66.3
15°	...	...	...	...	...	...	...	81.7	72.3	67.6
17°	...	...	...	...	...	...	...	...	67.5	64.2
19°	...	...	...	...	...	...	...	...	...	64.6

Note.—The correlation matrix Σ of the *WMAP*-NVSS CCF due to accidental alignments with the anisotropies produced at decoupling. Units are (μK counts)^2.

where T_i is the CMB map, N_j the NVSS map (described in the previous section), and the sums are over all pixel pairs separated by $\theta_k - \Delta\theta/2 < \theta < \theta_k + \Delta\theta/2$. The bin width $\Delta\theta$ is 2°. As before, we work at HEALPix resolution 5. Since we are working at large scales where the detector noise is negligible, we use the *WMAP* internal linear combination (ILC) map for the CMB (Bennett et al. 2003a). We limit residual foreground contamination by masking the map with the *WMAP* Kp0 galaxy mask and the *WMAP* source mask (Bennett et al. 2003b). The CMB weight w_i^T is the number of unmasked resolution-9 subpixels of the resolution-5 pixel i. The CCF is plotted in Figure 3. The CCF is insensitive to the form of the NVSS declination correction.

Assessing the significance of the CCF is complicated by the high degree of correlation between points. Accidental alignments between the NVSS map and the CMB fluctuations at the decoupling surface (which are uncorrelated with those generated by the late ISW) can produce spurious correlations. We quantified this uncertainty with Monte Carlo simulations, creating 500 realizations of the CMB sky drawn from the C_l^{TT} power spectrum for our fiducial model with our estimate of the NVSS-correlated late-ISW contribution subtracted. The covariance matrix Σ was calculated from the resulting CCFs, keeping the NVSS map fixed. Table 1 shows the $0^\circ < \theta < 20^\circ$ submatrix of Σ, showing that the CCF points are highly correlated. We define $\chi^2 = \delta C^T \Sigma^{-1} \delta C$, where $\delta C = \hat{C}^{NT} - C^{NT}$ is the difference between observed (eq. [11]) and model (eq. [8]) correlation functions, and we limit $\theta < 20^\circ$. This definition is reasonable since the simulations indicate that the elements of Σ are roughly Gaussian distributed. For the null model of no correlation ($C^{NT} = 0$), $\chi_0^2 = 17.2$. Since there are 10 degrees of freedom, this a 1.8 σ deviation.

How does the measured CCF constrain Ω_Λ? Rather than exploring the full parameter space, we assume a flat universe with fixed ω_b and explore the locus of values of Ω_m and h consistent with the measured location of the first acoustic peak of the CMB TT anisotropy power spectrum. The first peak position is set by the angular scale of the sound horizon at decoupling, θ_A, which Page et al. (2003) found to be $\theta_A = 0.^\circ6$. Percival et al. (2002) showed that $\theta_A \approx 0.^\circ85\Omega_m^{0.14}h^{0.48}$; this is the horizon angle degeneracy. The normalization A is varied to fix the amplitude of the first peak; from a fit to CMBFAST (Seljak & Zaldarriaga 1996) spectra we found $A \propto \Omega_m^{0.248}$ along the horizon degeneracy. The results are shown in Figure 4. The difference in χ^2 between models with $\Omega_\Lambda = 0$ (i.e., no correlation) and $\Omega_\Lambda = 0.68$ (the minimum, with $\chi^2_{\rm min} = 12.5$) is $\Delta\chi^2 = 4.7$. Since we are varying a single parameter, the significance is $(\Delta\chi^2)^{1/2}$; thus, $\Omega_\Lambda > 0$ is preferred at the 2.2 σ level.

That the significance of the Ω_Λ model (2.2 σ) is greater than the null model (1.8 σ) is not surprising, because the latter is not as sensitive a test. For example, consider a series of N samples $x_i = \epsilon + n_i$ where ϵ is a constant and n_i are independent Gaussian deviates with unit variance and zero mean. The optimal estimator for ϵ is the mean, $\bar{x}$, which has an expected detection significance of $\epsilon N^{1/2}$. The expected null χ^2 is $\langle \sum x_i^2 \rangle = N + N\epsilon^2$. For $N = 10$ and $\epsilon = (7/10)^{1/2}$, the χ^2 tends to be 17 (i.e., 1.8 σ), whereas the significance of $\bar{x}$ is on average $7^{1/2} = 2.6$ σ.

The *WMAP* team imposed a prior on the Hubble constant, $h > 0.5$, in determining the cosmological parameters (Spergel et al. 2003). While lower values of the Hubble constant would contradict a host of other experiments, especially the Hubble Key Project (Freedman et al. 2001), models with very low h and $\Omega_m \approx 1.3$ are marginally consistent ($\Delta\chi^2 = 4.9$) with the *WMAP* TT and TE angular power spectra. Since these universes are closed and matter dominated, the growth factor $D(a)$ grows faster than a, and $g(a)$ is better termed the linear growth *enhancement* factor. Thus, we would expect to observe an anticorrelation between the NVSS and CMB maps, since $dg/d\eta$ in equation (10) changes sign (see Fig. 1). For $\Omega_m = 1.28$ and $h = 0.33$, $\chi^2 = 24.2$ (with a bias of 2.7). Based on the cross-correlation analysis alone, this model is disfavored by more than 3 σ.

4. DISCUSSION

The recent acceleration of the universe because of dark energy should correlate large-scale CMB anisotropies with fluctuations in the local matter density through the late-time integrated Sachs-Wolfe effect. We have correlated the NVSS radio source catalog with the CMB anisotropies observed by the *WMAP* satellite, and find that $\Omega_\Lambda > 0$ is preferred at the 95% confidence level ($\Delta\chi^2 = 4.7$), considering statistical errors only. The statistical uncertainty is due to accidental alignments with the background primary anisotropies generated at decoupling. The likelihood peaks at $\Omega_\Lambda = 0.68$, consistent with the value derived from the CMB angular power spectrum.

The correlation between the NVSS source count and *WMAP* CMB maps appears robust. We interpret it as arising from the late ISW, but other effects could correlate the two maps. For instance, obscuration by dust clouds tends to reduce the number of sources observed in their direction. We cross-correlated

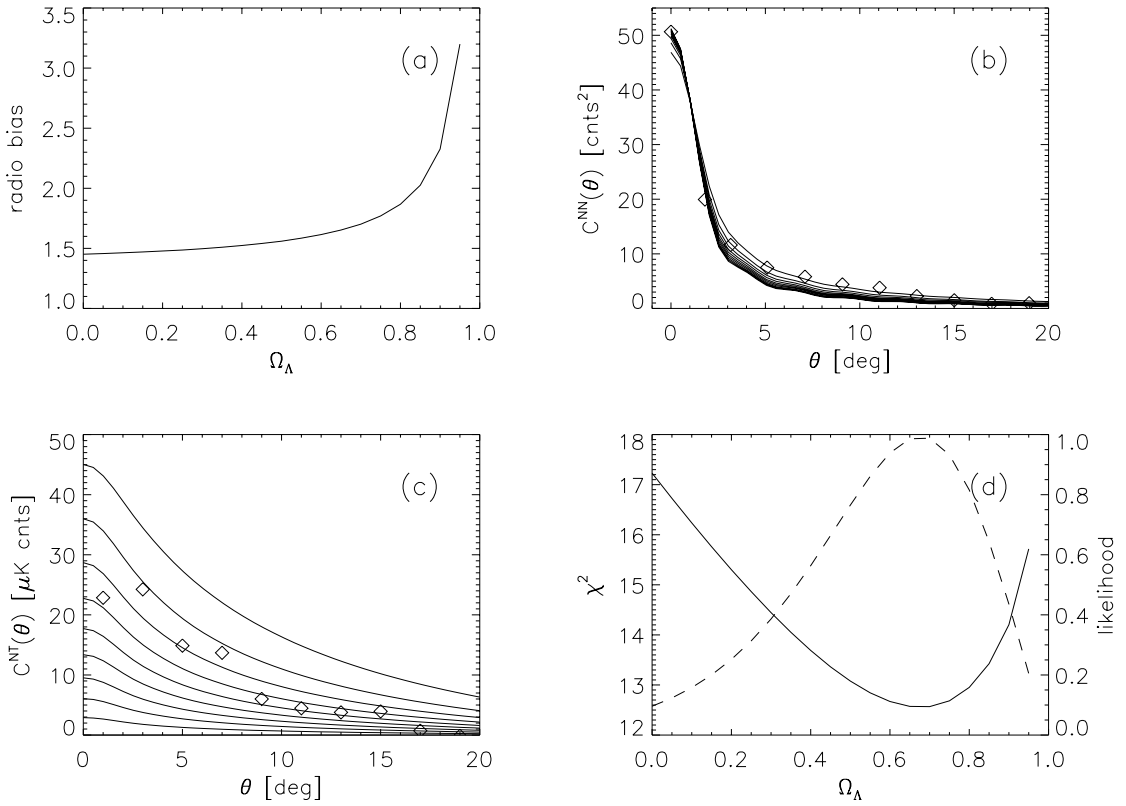

FIG. 4.—Effect of varying Ω_Λ on the CCF. In all panels we assume a flat universe with fixed ω_b, and trade off between Ω_Λ and h by keeping the combination $\Omega_m h^{3.4}$ constant; when $\Omega_\Lambda = 0$, $h = 0.48$. Panel *a* shows the inferred radio bias as a function of Ω_Λ. Panel *b* shows the bias-corrected NVSS ACF compared with the measured ACF. Panel *c* shows the predicted CCF for a range of values of Ω_Λ, compared with the measured CCF (*diamonds*). The amplitude of the predicted CCF is proportional to Ω_Λ, which is stepped in increments of 0.1 from 0.0 to 0.9. Panel *d* shows the χ^2 of the model CCF as a function of Ω_Λ. The χ^2 was computed using the first 10 points of the CCF ($0^\circ < \theta < 20^\circ$) and Table 1. The minimum $\chi^2_{\rm min}$ is 12.5 at $\Omega_\Lambda = 0.68$; at $\Omega_\Lambda = 0$, $\chi^2_0 = 17.2$. The dashed line is the likelihood $\propto \exp(-\chi^2/2)$. The 1 σ limits are $0.42 < \Omega_\Lambda < 0.86$.

the NVSS map with the $E(B-V)$ extinction map of Schlegel et al. (1998) and saw evidence for a small negative correlation at separations $\theta < 20^\circ$. However, since the extinction map is positively correlated with the CMB map because of dust emission, this effect has the wrong sign to mimic the late ISW. The extinction correction is estimated as $r_E(\theta) = \langle EN\rangle\langle ET\rangle/\langle EE\rangle$, where N, T, and E are the NVSS, CMB, and extinction maps, respectively, and $\langle XY\rangle$ denotes the correlation between maps X and Y evaluated at separation θ. We find a value of $r_E(0) \approx -4$ μK counts (compared to 22 μK counts for the CCF) and the correction is negligible for $\theta > 15^\circ$, except for a few glitches when $\langle EE\rangle$ crosses zero. Subtracting r_E from the CCF, we find the preferred value of Ω_Λ increases to 0.76; at the minimum $\chi^2_{\rm min} = 14.8$, and $\Delta\chi^2 = 6.1$.

A potentially more serious concern is that the correlation is due to microwave emission by the sources themselves. However, if this were the case then the CCF should have a similar angular profile to the ACF. Yet while the ACF falls steeply with increasing separation $[\hat{C}^{NN}(0^\circ)/\hat{C}^{NN}(3^\circ) \sim 5]$, the CCF does not $[\hat{C}^{NT}(0^\circ)/\hat{C}^{NT}(3^\circ) \sim 1]$. The lack of an enhanced signal in the zero lag CCF bin thus argues against any significant microwave emission from the NVSS radio sources. As another check, we replaced the ILC map with smoothed versions of the *Q*-, *V*-, and *W*-band maps, and found that the CCF was unchanged. This implies that the signal has a temperature spectrum, which rules out radio source contamination, which would have a $\sim\nu^{-2}$ spectrum.

We are indebted to Steve Boughn for significant and helpful discussions throughout the preparation of this paper. We also thank Hiranya Peiris, Uros Seljak, and Licia Verde for useful comments. The *WMAP* mission is made possible by the support of the Office of Space Sciences at NASA Headquarters and by the hard and capable work of scores of scientists, engineers, technicians, machinists, data analysts, budget analysts, managers, administrative staff, and reviewers.

REFERENCES

Bennett, C. L., et al. 2003a, ApJS, 148, 1
———. 2003b, ApJS, 148, 97
———. 2003c, ApJ, 583, 1
Boughn, S. P., & Crittenden, R. G. 2002, Phys. Rev. Lett., 88, 21302
———. 2004, Nature, 427, 45
Carroll, S. M., Press, W. H., & Turner, E. L. 1992, ARA&A, 30, 499
Condon, J. J., Cotton, W. D., Greisen, E. W., Yin, Q. F., Perley, R. A., Taylor, G. B., & Broderick, J. J. 1998, AJ, 115, 1693
Crittenden, R. G., & Turok, N. 1996, Phys. Rev. Lett., 76, 575
Dunlop, J. S., & Peacock, J. A. 1990, MNRAS, 247, 19 (DP90)
Fosalba, P., & Gaztanaga, E. 2004, MNRAS, in press (astro-ph/0305468)
Fosalba, P., Gaztanaga, E., & Castander, F. 2003, ApJ, 597, L89
Freedman, W. L., et al. 2001, ApJ, 553, 47
Górski, K. M., Hivon, E., & Wandelt, B. D. 1999, in Proc. MPA-ESO Cosmology Conference, Evolution of Large-Scale Structure: From Recombination to Garching (Enschede: PrintPartners Ipskamp)
Hinshaw, G., et al. 2003, ApJS, 148, 135
Page, L., et al. 2003, ApJS, 148, 233

Peebles, P. J. E. 1993, Principles of Physical Cosmology (Princeton: Princeton Univ. Press)
Peiris, H. V., & Spergel, D. N. 2000, ApJ, 540, 605
Percival, W. J., et al. 2002, MNRAS, 337, 1068
Perlmutter, S., et al. 1999, ApJ, 517, 565
Riess, A. G., et al. 1998, AJ, 116, 1009
Sachs, R. K., & Wolfe, A. M. 1967, ApJ, 147, 73
Schlegel, D. J., Finkbeiner, D. P., & Davis, M. 1998, ApJ, 500, 525
Scranton, R., et al. 2004, Phys. Rev. Lett., in press (astro-ph/0307335)
Seljak, U., & Zaldarriaga, M. 1996, ApJ, 469, 437
Spergel, D. N., et al. 2003, ApJS, 148, 175
Tegmark, M., de Oliveira-Costa, A., & Hamilton, A. 2003, Phys. Rev. D, 68, 123523
Verde, L., et al. 2003, ApJS, 148, 195